Tetragonal Y-doped zirconia: Structure and ion conductivity

A. Eichler
Institut für Materialphysik and Center for Computational Materials Science, Universität Wien, Sensengasse 8/12, A-1090 Wien, Austria
(Received 22 May 2001; published 3 October 2001)

Zirconia is of great industrial importance as support for catalysts and as ion conductor. Especially when mechanical stability is needed in environments with varying temperature the tetragonal modification is superior, because of its high resistivity against physical shocks and thermal stresses. In this study density functional theory is used to investigate the interaction between Y impurities and oxygen vacancies and to develop in this way a structural model for Y-doped zirconia. For every two Y defects an O vacancy is formed at a distance of about 4.11 Å to each dopant. An activation energy for ion conductivity of 0.87 eV is calculated in very good agreement with experimental findings.

DOI: 10.1103/PhysRevB.64.174103 PACS number(s): 61.72.Ji, 66.30.Dn, 71.15.Mb

I. INTRODUCTION

Zirconia is widely used as support material in catalysis. A second important property used in many applications is its ion conductivity, mediated by oxygen vacancies. The concentration of vacancies can be varied by dopants such as ceria or yttria. These dopants influence also the crystal structure of zirconia. Pure zirconia has a monoclinic structure up to a temperature of about 1446 K, where it changes to the tetragonal modification. For temperatures higher than 2643 K zirconia adopts a cubic fluorite structure. Yttrium doping can be employed to partially or completely stabilize the tetragonal and cubic modification, even at room temperature (PSZ: partially stabilized zirconia; FSZ: fully stabilized zirconia, Y-content above approximately 8 mol %). PSZ (with an Y content of about 2–6 mol %) has the advantage of high resistivity against physical shocks and thermal stresses. While cubic zirconia has been studied in the past quite thoroughly, information on the tetragonal modification is scarce. In this study, we examine the bulk phase of tetragonal zirconia, the structure around oxygen vacancies and yttrium dopants, as well as the oxygen ion conductivity on the basis of density functional theory (DFT).

II. THEORY

The calculations are performed using the Vienna *ab initio* simulation package VASP (Refs. 1,2) which is a density-functional-theory (DFT) code, working in a plane wave basis set. Electron-ion interaction is described using the projector augmented wave method[3,4] with plane waves up to an energy of $E_{\mathrm{cut}}=250$ eV. For exchange and correlation the functional proposed by Perdew and Zunger[5] is used, adding (nonlocal) generalized gradient corrections (GGA).[6] For the primitive bulk cell (containing two zirconium and four oxygen ions) Brillouin zone sampling was performed on a dense $\vec{k}$-point mesh of $15\times15\times11$ points. However, for the larger supercells used throughout most of the calculations we restricted the $\vec{k}$-point sampling to one single (off symmetry) point at $(\frac{1}{4},\frac{1}{4},\frac{1}{4})$. To determine the diffusion barriers, transition states were determined using the nudged elastic band method (NEB).[7,8]

III. PURE ZIRCONIA

As a starting point for our investigation we used the work of Jomard *et al.*[9] where several bulk phases of zirconia have been investigated with the same method.[1] We repeated the structural optimization for the tetragonal phase starting from the geometry reported in Ref. 9 within the setup used here. The results are compiled in Table I together with the experimental values.

The density of states (DOS) of tetragonal ZrO_2 is displayed in the top panel of Fig. 1. Starting from the lowest energies, the first states are the zirconium $4s$ and $4p$ states (at around -48 and -26 eV; not shown in the graph) followed by the O-$2s$ states. The oxygen p band, completely filled by the transfer of two Zr d electrons per O ion is the highest occupied energy band (valence band). The empty Zr d band represents the conduction band of this semiconductor and is separated by an energy gap of 4.21 eV from the valence band. Experimentally a direct band gap of 4.2 eV (electron energy loss spectroscopy)[12] and 5.78 eV (vacuum-ultraviolet spectroscopy)[13] has been determined.

For all further investigations we increase the size of our basis cell, so that small amounts of impurities and/or vacancies can be examined. The primitive cell was multiplied by a factor of three in x and y directions and doubled in the z direction leading to an approximately cubic supercell of 10.94 Å×10.94 Å×10.57 Å containing 36 ZrO_2 formula units. With this setup, the smallest possible Y content that can be achieved is Y:Zr=1:35 (equivalent to 1.4 mol % or 2.6 mass % Y_2O_3). In a similar manner Stapper *et al.*[14] investigated Y-doped cubic zirconia, so that a direct comparison between cubic and tetragonal zirconia is possible.

TABLE I. Lattice constant a, c/a ratio and distortion parameter d_z for tetragonal zirconia compared to experimental values from Refs. 10,11.

	Calc.	Exp.
a	3.645	3.605
c/a	1.451	1.437
d_z	0.054	0.065

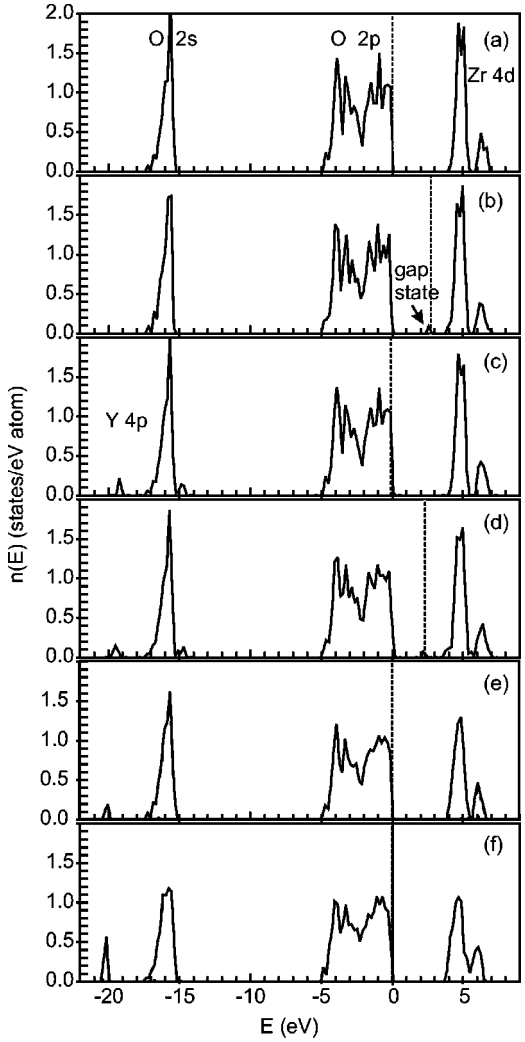

FIG. 1. Density of states (DOS) for tetragonal zirconia: pure (a), with a single oxygen vacancy (b), with a single Y impurity (c) and with an O vacancy and a Y impurity (d) per 36 formula units ZrO_2. Panels (e) and (f) show DOS for the optimized structures at 2.9 mol and 5.9 mol %. The energy zero is set to the top of the O-2p band, the dashed line indicates the Fermi level.

IV. ISOLATED IMPURITIES

A. Oxygen vacancy

The formation of an isolated O vacancy in pure zirconia leads to a situation where the O p band can no longer hold all Zr-d electrons. As a consequence a gap state accommodating the excess electrons appears [see Fig. 1(b)]. This gap state is visualized in real space in Fig. 2(a): Zr-d orbitals extending into the position of the O vacancy and hence conserving the local charge (2^-) of the missing O ion at its former position. The distortion pattern due to the removal of the oxygen atom is sketched in Fig. 3. All surrounding ions move towards the vacancy to reduce its size; the two Zr ions by 0.08 Å, the O ions slightly more (up to 0.13 Å). However, the two electrons captured in the vacancy prevent a more pronounced distortion. Nevertheless, the energy gain due to the relaxation of the ions is 0.22 eV.

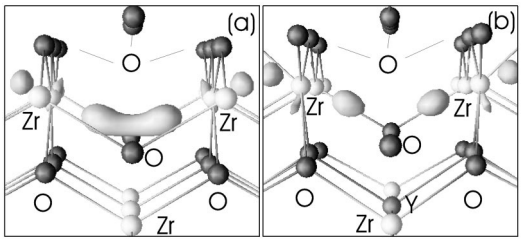

FIG. 2. Charge-density iso-surface of gap states, due to the formation of an oxygen vacancy in pure zirconia (a) and with a single Y impurity (b).

Charged vacancies. When we remove not only a neutral oxygen atom, but also the additional electrons completely or partially, which are localized at this ion, then the remaining cell is charged: this charge is $+1$, if an O^- ion, and $+2$, when an O^{2-} -ion is removed from the cell. The corresponding vacancies are then called F $(Farb)^+$ or F^{++} center. This charging of the cell implies several corrections to the energy: on one hand the interaction of point charges (due to the periodic boundary conditions) has to be considered and on the other hand a correction term for varying Fermi levels has to be introduced. In addition to that, spin-polarization has to be taken into account for the singly charged cell. The formation energy of a vacancy (dependent on the charge of the cell q and the Fermi level ε_F with respect to the valence band maximum E^{val}) can be calculated according to

$$E_f(q,\varepsilon_F)=E_{tot}-E_{tot}^{ref}+q\cdot\varepsilon_F-E_c(q) \tag{1}$$

with the total energy from the calculation E_{tot}, the reference energy for neutral cells E_{tot}^{ref} and finally a correction term $E_c(q)$ for the Coulomb interaction of point charges

$$E_c(q)=-(qe)^2\frac{\alpha}{a_0\varepsilon_0}. \tag{2}$$

α stands for Madelung's constant of the cell, a_0 for the lattice parameter, and ε_0 for the dielectric constant of tetragonal ZrO_2, for which we took a value of $\varepsilon_0=39.8$ from the literature.[15] This correction term results in an up shift in energy by 47(190) meV for singly (doubly) charged cells. For the reference energy of the uncharged system we take $E_{tot}(ZrO_2)-\frac{1}{2}E_{tot}(O_2)$. In that way the formation energy describes the energy cost for creating an oxygen vacancy and forming at the same time half an O_2 molecule. Formation energies according to these equations are visualized in Fig. 4 as function of the position of the Fermi level.

An obvious result from Fig. 4 is, that singly charged F^+-centers are always unstable with respect to a pairwise decay into a doubly charged F^{++} and a neutral F center. The corresponding result has been obtained previously for cubic zirconia.[14] Neutral F centers exist only for rather high values of ε_F, which can be achieved by dopants, which induce a surplus of electrons (Nb, ...). When yttria is used as dopant, as we assume in the present study, only F^{++} centers will be realized.

In the case of charged F centers the structural distortions around the vacancies are much more pronounced. The sur-

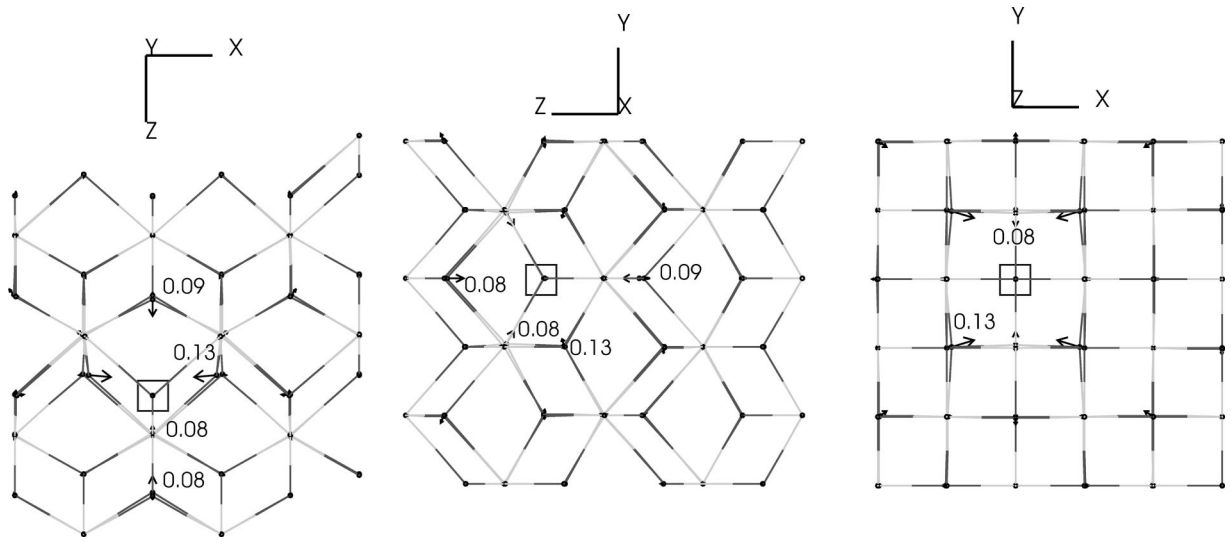

FIG. 3. Sketch of the optimized structures of ZrO_2 with a single O vacancy. Arrows indicate the direction of distortion, a square denotes the positions of the O vacancy. The numbers describe the distortion (in Å) with respect to the ideal bulk structure.

rounding O^{2-} ions are no longer repelled by the captured electrons, but move closer (up to 0.22/0.33 Å) towards the F^+/F^{++} center. The Zr ions, on the other hand, are now repelled from the vacancy and move 0.09 (0.22) Å from the singly (doubly) charged defect. These values are again in nice agreement with what was obtained for cubic zirconia.[14] The structural effects are accompanied by energy gains (per supercell) of 1.0 and 3.3 eV for the singly and doubly charged cell, respectively.

Table II finally compiles the formation energies, energy gaps and positions of gap states for the three F centers. For the F^+ center also results for a spin-polarized calculation are given.

B. Yttrium dotation

Yttrium-doping induces additional states in the DOS, located slightly above the corresponding zirconia states [see, Fig. 1(c)]. Since yttrium possesses one *d*-electron less than zirconium, the oxygen *p*-band is no longer fully occupied. Hence, the Fermi level is pinned at the upper edge of the valence band. Similar to the oxygen vacancies discussed above, the Y defect can carry charge. However, in this case the difference in formation energies [according to Eq. (1)] is only 70 meV (at $\varepsilon_F=0$). This implies, that already for a Fermi-level of 70 meV above the valence band maximum, charged Y defects are favored. Relaxation of ionic coordinates (see Fig. 5) leads to an energy gain of 0.83 eV for the neutral defect. The distance of the surrounding O-ions from the Y-ion increases by approximately 0.16 Å compared to the Zr-O distances. The reason for that is on one side the greater ionic radius of yttrium and on the other side the smaller positive charge on the Y^{3+} (than on Zr^{4+}) which is less attractive to the doubly negative charged oxygen ions.

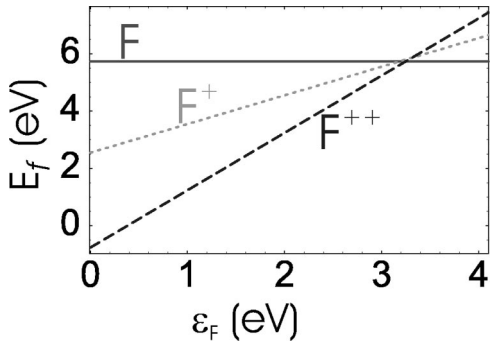

FIG. 4. Formation energy (E_F) of neutral, singly and doubly charged F centers in ZrO_2 as a function of the Fermi level (ε_F) with respect to the valence band maximum.

V. DEFECT INTERACTION

Based on the calculations so far, we got some ideas on the influence of impurities on the structure in the surrounding and on the energetics. In the following we investigate the interaction between different defects.

A. Y dopant and O vacancy

(Single) yttrium doping reduces the total number of electrons, comparable to the situation of the singly charged cell, discussed above. Creating an oxygen vacancy in such a doped environment results in a singly occupied gap state.

TABLE II. Formation energy E_f for $\varepsilon_F=0$ [according to Eq. (1)], energy gap and position of the gap-state with respect to the valence band maximum in eV for F centers. F^+ (spin) refers to a spin-polarized calculation.

Vacancy	E_f	Gap	Gap state
F	5.73	4.07	2.82
F^+	2.69	4.16	3.31
F^+ (spin)	2.55	4.14	2.97
F^{++}	-0.76	4.11	

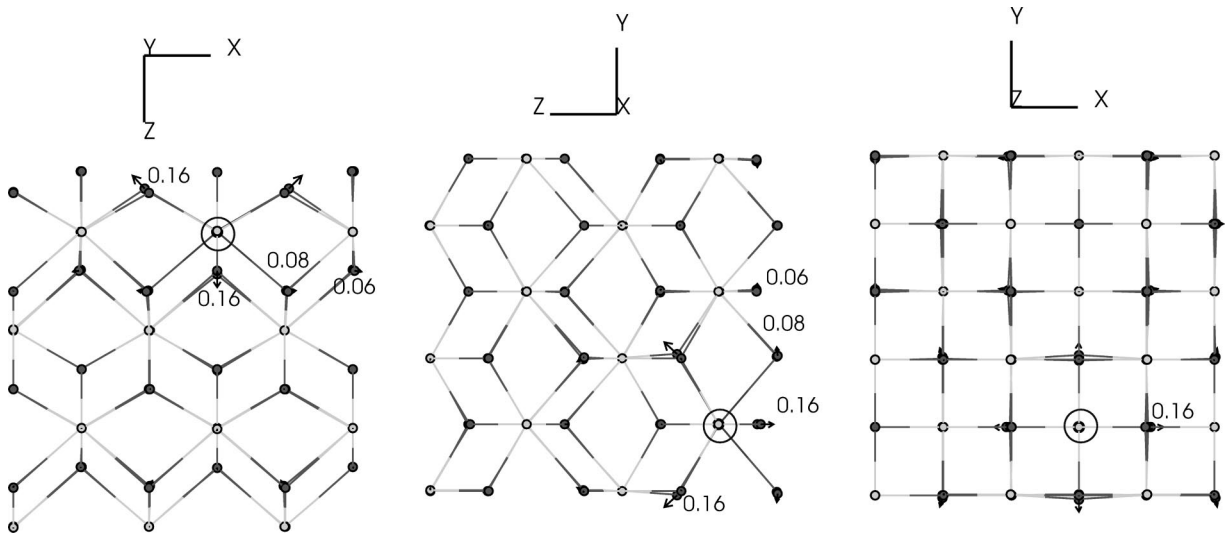

FIG. 5. Sketch of the optimized structure of ZrO_2 with a single Y defect. Arrows indicate the direction of distortion, a circle denotes the positions of the Y ion. The numbers describe the distortion (in Å) with respect to the ideal bulk structure.

This reduces the vacancy formation energy (compared to the case without Y dopant) approximately by the energy, that is necessary to raise one electron from the valence band into the gap state (see Table II). Also the energy gap (4.15 eV) and the position of the gap state (3.36 eV from E^{val}) remains almost unchanged compared to the case with the singly charged cell. Since we know already, that F^+ centers are unstable, it suggests itself to repeat the calculation also for an F^{++} center, i.e., in a singly charged cell. This results again in an additional energy gain of around 0.7 eV. In order to quantify the interaction between Y ion and O vacancy, we define a binding energy E_b as

$$E_b = E[Y + \mathrm{vac}] - [E[\mathrm{vac}] + E[Y] - E[\mathrm{ZrO_2}]], \qquad (3)$$

where $E[\mathrm{vac}], E[Y]$, and $E[\mathrm{ZrO_2}]$ describe the total energies of the isolated defects and of pure zirconia, all calculated for the same unit cell. For the defects, we took the energies from the corresponding charged calculations (including Coulomb corrections). Figure 6 illustrates this binding energy as a function of the Y-vacancy distance (negative values of E_b describe attractive interaction.). In both cases (for F^+ and F^{++} centers) a preference for distances around 4.0–4.5 Å, with a minimum at 4.11 Å is obvious. This result agrees with the experimental findings[16] and is also consistent with the preference of next nearest neighbor sites for vacancies over nearest neighbor sites in cubic zirconia, which has been found experimentally,[17,18] as well as theoretically.[14,19] Also the binding energies for cubic zirconia given in Ref. 14 ($E_b^{NN} = -0.10$ eV, $E_b^{NNN} = -0.44$ eV) fit well to the values reported above.

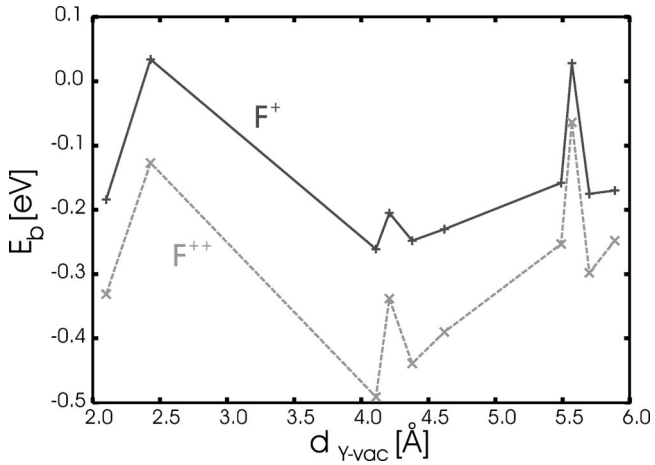

FIG. 6. Binding energy between Y impurity and F center as a function of the distance.

The structural modifications (for the optimal Y-vac distance) are shown in Fig. 7. The relaxations around the vacancy are very similar to those around vacancies with corresponding charge in the pure system. Only the oxygen ion next to the Y ion moves closer towards the vacancy (0.24 Å for the F^+, 0.43 Å for the F^{++} center), since it is less attracted by the Y^{3+} ion.

B. Y-Y interaction

In a next step, we investigate the interaction between two Y defects. Two Y ions within our supercell is equivalent to a doping of 2.9 mol % Y_2O_3 (5.6 mol % $YO_{1.5}$ or 5.1 mass % Y_2O_3). Y-Y binding energies, calculated according to Eq. (3), are compiled in Table III. For the neutral Y-Y pair we used the neutral isolated Y defect as reference system, for the doubly charged cell the charged defect.

The results for both calculations are consistent: defects in nearest neighbor distance (for the optimized structure, compare Fig. 8) are preferred compared to such with a distance of 5.15 Å, while Y ions at maximal distance are even lower in energy. However, these energy differences between various configurations are only rather small compared to the differences in the Y-O interaction energies.

C. Y-Y-vacancy trimers

From the point of view of charge neutrality this configuration is what is to be expected: one oxygen vacancy (F^{++})

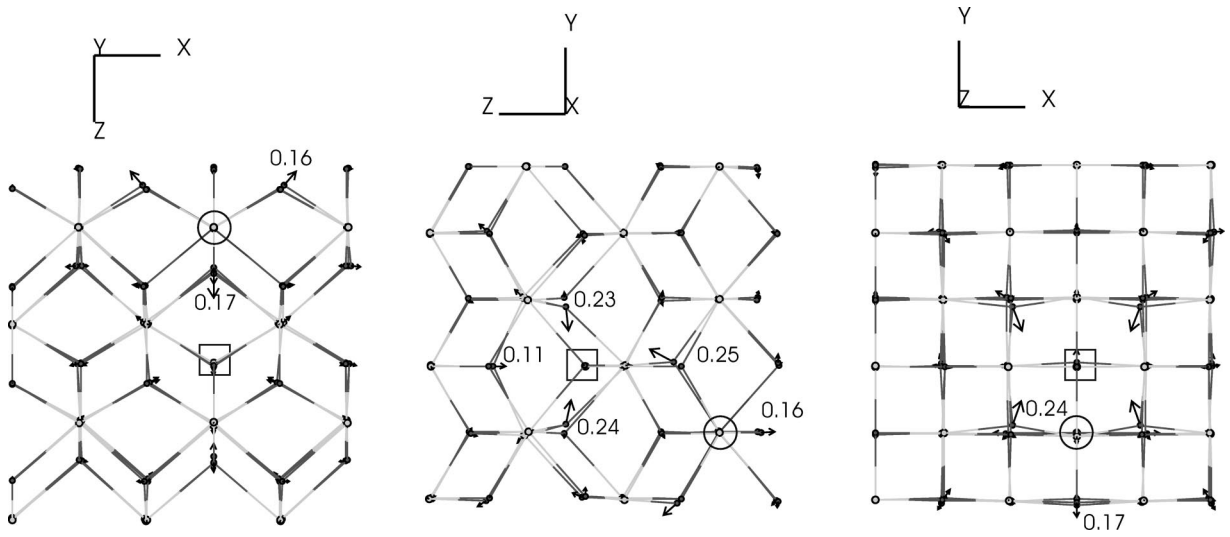

FIG. 7. Sketch of the optimized structure for an oxygen vacancy and a Y defect in tetragonal ZrO_2. Arrows indicate the direction of distortion, circles and squares denote the positions of Y impurities and O vacancies, respectively. The numbers (in Å) describe the distortion with respect to the ideal bulk structure.

compensates for two Y defects. Also for this situation, we investigated several probable configurations, always taking into account the results from the previous calculations. The sum of the separate interaction energies for isolated defects from Fig. 6 and Table III gives already a reasonable estimate for the stability of each configuration. These approximate binding energies (E_b^{approx}) together with the calculated values for various possible Y-Y-F^{++} trimers are compiled in Table IV.

The dominant contribution to the binding energy comes from the Y-vacancy interaction: for the most stable configuration both Y ions have the optimal distance of 4.11 Å to the oxygen vacancy. These Y-Y-vacancy triangles are oriented symmetrical along the (001) axes, inducing a distortion pattern as sketched in Fig. 9. As in the previous cases, a superposition of the distortion patterns of the isolated defects (Y,F^{++}) leads to a good description of the total effect: O ions move by about 0.14 Å away from the Y defects, O ions around the vacancies move by about 0.33 Å towards the defect, while Zr ions increase their distance to the vacancy by $\sim$0.15 Å. Solely, that oxygen atom in the immediate vicinity of the vacancies and impurities moves by 0.62 Å towards the two sevenfold coordinated Zr ions.

D. ZrO_2 with 5.9 mol % yttria

Finally we also investigate a configuration with an yttria content of 5.9 mol % percent (11.1 mol % $YO_{1.5}$, 10.3 mass % Y_2O_3) In this concentration regime, the tetragonal phase is still stable at room temperature, but we are already close to the tetragonal-cubic phase transition. Again we use the information accumulated so far: we assume the existence of Y-Y-F^{++} trimers, as we have calculated above (see Table IV) and optimize the relative position of such triangles within the supercell. The characteristic distances for the investigated configurations together with the binding energy between two such triangles are compiled in Table V.

The most favorable configuration (with a binding energy of -0.81 eV) is also that with the highest symmetry (see Fig. 10). The Y-Y-F^{++} triangles are oriented such that the distances between the oxygen vacancies and those between the Y defects and the vacancy of the second trio are maximized. Both Y-Y-F^{++} triangles are oriented parallel to the (001) axes, but perpendicular to each other: while one of them is lying in the (x,z), the second one is located within the (y,z) plane. In this configuration all undercoordinated (sevenfold) Zr ions are within the same (x,y) plane, with the O vacancies being alternatively below and above that plane. This leads to a situation for which 4 out of 9 Zr ions in that plane are undercoordinated. This undercoordination induces stronger bonds with all other neighboring O atoms and hence reduces the average interplane distance of (x,y) Zr and O planes. Hence, although the cell geometry and shape was kept constant during the relaxation the interlayer distance is

TABLE III. Binding energy between two Y impurities in zirconia at a distance of $d_{Y\text{-}Y}$ calculated in neutral and doubly charged cells.

d_{Y-Y} (Å)	E_b^0 (eV)	E_b^{--} (eV)
3.65	+.05	0.12
5.15	+.10	0.18
7.38	−.02	0.03

TABLE IV. Binding energy of Y-Y-F^{++} trimers and characteristic distances (for the undistorted system) in Å.

$d_{Y_1-Y_2}$ (Å)	d_{Y_1-v} (Å)	d_{Y_1-v} (Å)	E_b^{approx} (eV)	E_b
3.65	4.38	4.38	−0.76	−0.66
5.15	4.38	4.38	−0.70	−0.34
7.38	4.38	4.11	−0.90	−0.85
3.65	4.11	4.11	−0.86	−0.93

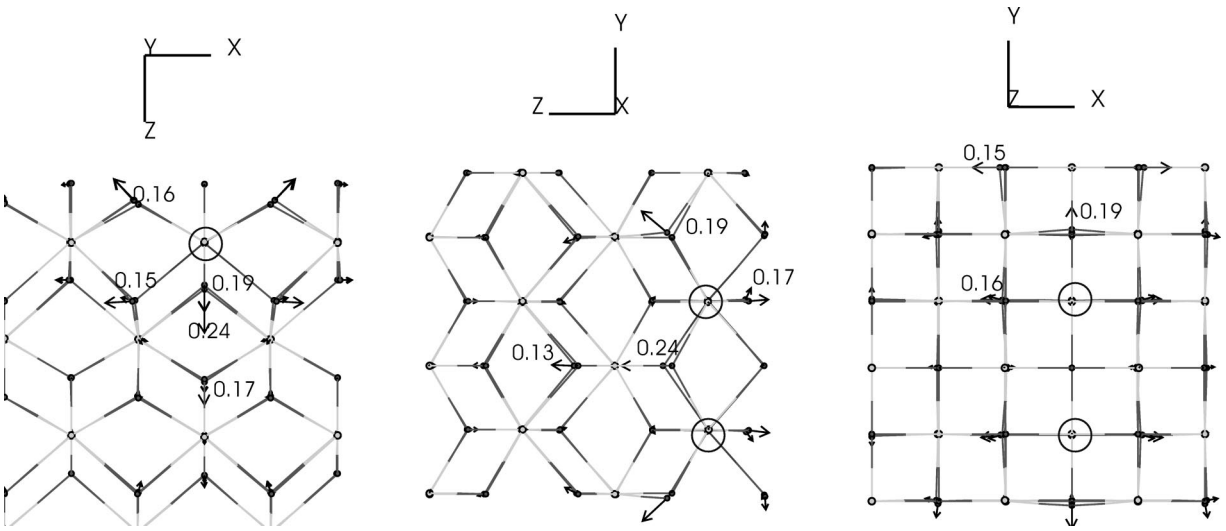

FIG. 8. Sketch of the optimized structures of two Y impurities in ZrO_2. Arrows indicate the direction of distortion, the circles denote the positions of the Y impurities. The numbers (in Å) describe the distortion with respect to the ideal bulk structure.

reduced from 1.322 Å in tetragonal zirconia to 1.294 Å. Cubic zirconia (at the same lattice constant) has an interlayer distance of 1.289 Å. Also the buckling within the oxygen layer is reduced from the ideal tetragonal value of $d_z \cdot c/a \cdot a = 0.29$ Å (see Table I) to 0.22 Å. Both trends are a clear indication for a beginning tetragonal to cubic transformation.

VI. ION CONDUCTIVITY

A. Pure zirconia

The ion conductivity in zirconia is mediated via oxygen vacancies. Since the local environment is different around charged and noncharged F centers, different diffusion barriers are expected. In pure tetragonal zirconia two distinct directions are possible for the ion (vacancy) current: within the (x,y) plane along the (110) [or $(\bar{1}10)$] direction, or perpendicular to this plane in the (001) direction (for the directions, please compare the sketches for ion diffusion in Y-doped ZrO_2 in Fig. 11). For both directions the O-O distance is very similar: 2.640 Å within the (x,y) plane and 2.644 Å in the direction perpendicular to that plane. Nevertheless, the diffusion barriers (compiled in Table VI) differ significantly. The barrier is in both cases determined by a configuration (transition state) for which the oxygen ion moves between two Zr ions towards its new position. In the situation with the movement in (001) direction these Zr ions have an ideal bulk distance of 3.645 Å, while this distance is slightly (0.05 Å) larger for diffusion within the (x,y) plane. This tiny difference is the reason for the lower diffusion barrier in (110) direction. The higher barrier for the uncharged F centers comes from the strong repulsion between the negatively

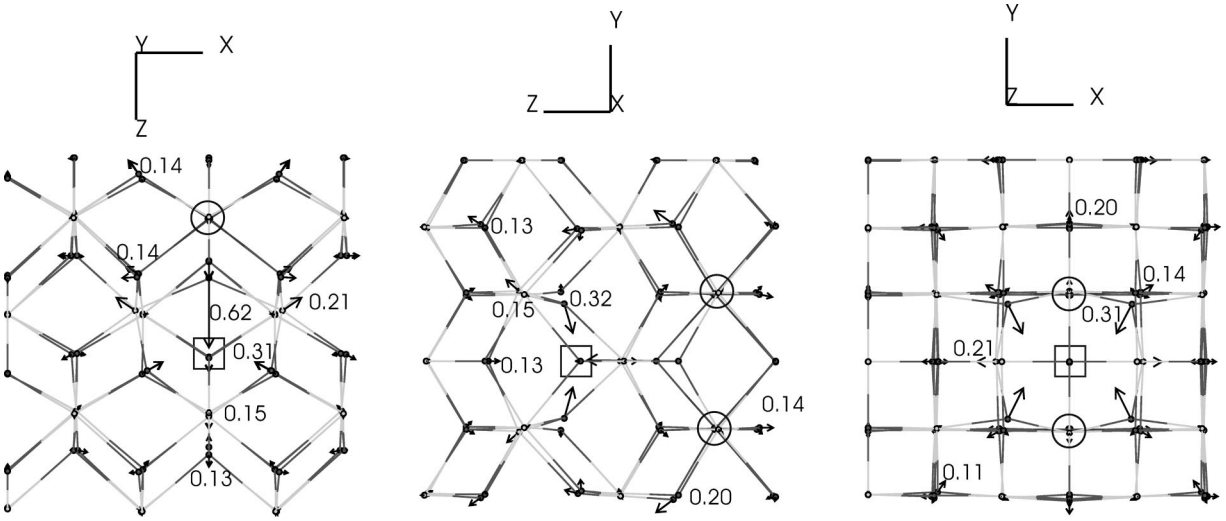

FIG. 9. Sketch of the optimized structures of a Y-Y-F^{++} trimer in ZrO_2. Arrows indicate the direction of distortion, circles and squares denote the positions of Y impurities and O vacancies, respectively. The numbers describe the distortion with respect to the ideal bulk structure.

TABLE V. Binding energy E_b (in eV) between two Y-Y-F^{++} trimers and characteristic distances (for the undistorted system) between vacancies ($v_{1,2}$) and Y ions (Y_{1-4}) in Å.

v_1 v_2	v_1 Y_3	v_1 Y_4	v_2 Y_1	v_2 Y_2	Y_1 Y_3	Y_1 Y_4	Y_2 Y_3	Y_2 Y_4	E_b
3.65	5.49	5.49	5.49	5.49	3.65	5.15	5.15	3.65	0.75
5.15	5.49	7.53	7.53	5.49	5.15	5.15	3.65	5.15	0.49
6.13	4.38	4.38	5.70	6.76	6.42	6.42	7.38	7.38	−0.43
8.01	6.76	6.76	6.76	6.76	7.38	7.38	7.38	7.38	−0.81

charged O ion and the electrons captured in the vacancy, which exchange their position at the barrier.

B. Y-doped zirconia

For the Y-doped system the situation becomes much more complicated. Oxygen/vacancy positions are no longer equivalent. The stability of different vacancy positions—as we have shown in the previous sections—depends strongly on the Y-F^{++} distances. So it is no longer sufficient to calculate the barrier for vacancy diffusion from one position to the next, but we have to calculate the barriers between several vacancy positions until the vacancy arrives finally at a position equivalent to the starting point. Starting from the optimal configuration described in Sec. V C, there are again two possible pathways for the vacancy: within the (x,y) plane, or perpendicular to it (compare the sketches in Fig. 11). In the first case the pathway is longer—the vacancy encounters six positions until it is again in a position equivalent to the starting configuration, compared to only four inequivalent positions during diffusion in (001) direction (see Table VII). However, since the pathway parallel to the (110) direction is symmetrical, only four positions are inequivalent and the computational effort remains the same. Already on the basis of the configurations along the pathways (Table VII) we expect a smaller barrier for diffusion within the (x,y) plane, since in the second case the vacancy has to

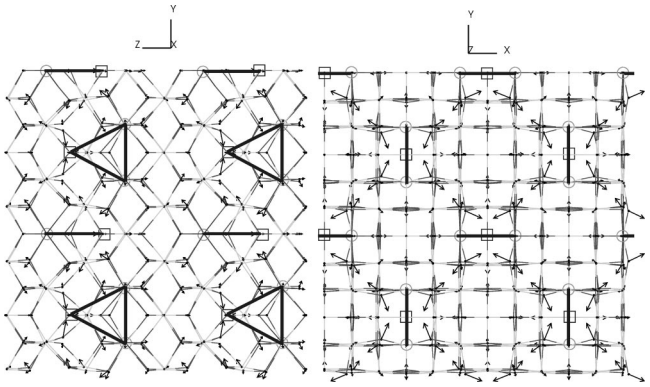

FIG. 10. Sketch of the optimized structures of tetragonal ZrO_2 with 5.9 mol % yttria content. Arrows indicate the direction of distortion, circles and squares denote the positions of Y impurities and O vacancies, respectively. The Y-Y-F^{++} trimers are marked by triangles. The cell has been doubled in each direction for better visualization.

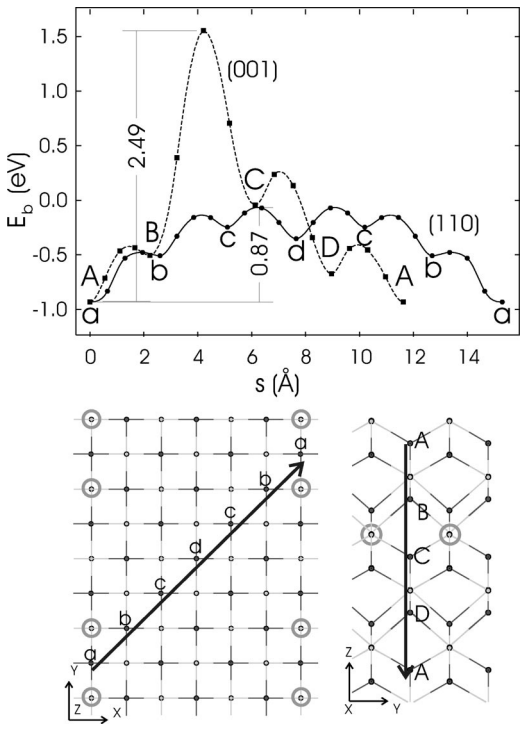

FIG. 11. Y-Y-F^{++} interaction energies for vacancy diffusion in Y-doped zirconia along the (011) (full line) and the (001) direction (dashed line) as a function of a reaction path coordinated *s*. Calculated values are indicated by points, smooth lines are drawn on the basis of these points and corresponding tangents.

come very close to the Y ions—a configuration which is energetically unfavorable (see Fig. 6).

In Fig. 11 we have completed the pathways by the barriers between successive vacancy positions. Diffusion along (001) is dominated by a huge barrier between position 2 and 3, where the oxygen ion (the vacancy) has to pass between the two Y ions. This situation is comparable to the diffusion along (001) discussed for pure zirconia, with the additional complication that the ionic radius of Y^{3+} is bigger than that of Zr^{4+}, so that the gap between the two ions is even smaller, and hence the barrier higher.

Diffusion along (110) on the other hand is activated (for 2.9 mol % Y_2O_3) by 0.87 eV. This barrier comes roughly from the energy difference between the most and less favorable vacancy position along the pathway plus the diffusion barrier of an F^{++} center along the (110) direction. Experimentally determined values for the diffusion barrier (at the same Y content) range between 0.80 and 0.96 eV.[20–24] The most recent work by Capel and co-workers[24] distinguished between contributions at grain-boundaries and barriers in the

TABLE VI. Diffusion barriers (in eV) for charged and uncharged vacancies in pure zirconia along the (110) and (001) directions.

	F	F^{++}
(110)	1.35	0.22
(001)	1.43	0.61

TABLE VII. Binding energies E_b (in eV) for the vacancy positions that are encountered during diffusion pathways along (110) and (001) directions in Y-doped zirconia (compare Fig. 11).

	(110) E_b	(001) E_b
a/A	−0.93	−0.93
b/B	−0.51	−0.50
c/C	−0.35	−0.04
d/D	−0.25	−0.67

tetragonal bulk and reports a bulk barrier of 0.86 eV in excellent agreement with our result.

So, we find that the diffusion barrier in the doped material is determined by two contributions: a site-to-site diffusion barrier around 200 meV for diffusion within the (110) plane and the interaction energy between the dopants and the position of the vacancies. The latter part depends strongly on the arrangement and amount of Y-ions in the zirconia matrix. This explains the observed dependency of the ion conductivity on Y doping and temperature.[23]

VII. SUMMARY

Summarizing we have investigated the bulk properties of tetragonal zirconia—in its pure form and for various contents of yttria. On the basis of these first principles calculations we have demonstrated the following points.

F^{++} centers are stable except for high Fermi energy, whereas F^{+} centers are always unstable with respect to a pairwise decay into a doubly charged F^{++} and a neutral F center.

For every two Y impurities an oxygen vacancy is created at a distance of 4.11 Å from both Y ions. These Y-Y-F^{++} trimers are oriented symmetrically along the (001) axis.

For higher yttria contents these Y-Y-F^{++} trimers are arranged such that the distance between the vacancies is maximized. Already for yttria contents of 5.9 mol % a clear tendency for the tetragonal to cubic phase transition is observable.

Vacancy diffusion occurs only perpendicular to the (001) axes. In clean zirconia diffusion of F (F^{++}) centers is activated by 1.35 (0.22) eV. Y doping (yttria content of 2.9 mol %) increases the activation energy to 0.87 eV in perfect agreement with measured values.[20–24]

ACKNOWLEDGMENTS

Calculations have been performed on the Cray T3E at the John v. Neumann Institute for Computing in the Forschungzentrum Jülich. Special thanks to G. Kresse and J. Hafner for helpful comments and discussions.

[1] URL http://cms.mpi.univie.ac.at/vasp/
[2] G. Kresse and J. Furthmüller, Phys. Rev. B **54**, 11 169 (1996); Comput. Mater. Sci. **6**, 15 (1996).
[3] P.E. Blöchl, Phys. Rev. B **50**, 17 953 (1994).
[4] G. Kresse and D. Joubert, Phys. Rev. B **59**, 1758 (1998).
[5] J.P. Perdew and A. Zunger, Phys. Rev. B **23**, 5048 (1981).
[6] J.P. Perdew, J.A. Chevary, S.H. Vosko, K.A. Jackson, M.R. Pederson, D.J. Singh, and C. Fiolhais, Phys. Rev. B **46**, 6671 (1992).
[7] G. Mills, H. Jónsson, and G.K. Schenter, Surf. Sci. **324**, 305 (1995).
[8] A. Ulitsky and R. Elber, J. Chem. Phys. **92**, 1510 (1990).
[9] G. Jomard, T. Petit, A. Pasturel, L. Magaud, G. Kresse, and J. Hafner, Phys. Rev. B **59**, 4044 (1999).
[10] C.J. Howard, R.J. Hill, and B.E. Reichert, Acta Crystallogr., Sect. B: Struct. Sci. **44**, 116 (1988).
[11] G. Teufer, J. Appl. Crystallogr. **15**, 1187 (1962).
[12] D.W. McComb, Phys. Rev. B **54**, 7094 (1996).
[13] R.H. French, S.J. Glass, F.S. Ohuchi, Y.-N. Xu, and W.Y. Ching, Phys. Rev. B **49**, 5133 (1994).
[14] G. Stapper, M. Bernasconi, N. Nicoloso, and M. Parrinello, Phys. Rev. B **59**, 797 (1999).
[15] A. Dwivedi and A.N. Cormack, Philos. Mag. A **61**, 1 (1990).
[16] P. Li, I.-W. Chen and J.E. Penner-Hahn, Phys. Rev. B **48**, 10 063 (1993); **48**, 10074 (1993); **48**, 10082 (1993).
[17] D.N. Argyriou, M.M. Elcombe, and A.C. Larson, J. Phys. Chem. Solids **57**, 183 (1996).
[18] C.R.A. Catlow, A.V. Chadwick, G.N. Greaves, and L.M. Moroney, J. Am. Ceram. Soc. **69**, 272 (1986).
[19] M.S. Khan, M.S. Islam, and D.R. Bates, J. Mater. Chem. **8**, 2299 (1998).
[20] S. Ikeda, O. Sakurai, K. Uematrsu, N. Mizutani, and M. Kato, J. Mater. Sci. **20**, 4593 (1985).
[21] N. Bonanos and E.P. Butler, J. Mater. Sci. Lett. **4**, 561 (1985).
[22] S.P.S. Badwal, Solid State Ionics **52**, 23 (1992).
[23] M. Filal, C. Petot, G. Petot-Ervas, M.C. Amamra, J.L. Carpentier, and J.L. Dellis, J. Phys. IV **3**, 1463 (1993).
[24] F. Capel, C. Moure, P. Duran, A.R. Gonzalez-Elipe, and A. Caballero, J. Mater. Sci. **35**, 345 (2000).